



Theoretical calculations of excited rovibrational levels of HD. Term values and transition probabilities of VUV electronic bands

Hervé Abgrall, Evelyne Roueff

► To cite this version:

Hervé Abgrall, Evelyne Roueff. Theoretical calculations of excited rovibrational levels of HD. Term values and transition probabilities of VUV electronic bands. *Astronomy and Astrophysics - A&A*, 2006, 445, pp.361-372. 10.1051/0004-6361:20053694 . hal-03785956

HAL Id: hal-03785956

<https://hal.science/hal-03785956>

Submitted on 27 Sep 2022

HAL is a multi-disciplinary open access archive for the deposit and dissemination of scientific research documents, whether they are published or not. The documents may come from teaching and research institutions in France or abroad, or from public or private research centers.

L'archive ouverte pluridisciplinaire **HAL**, est destinée au dépôt et à la diffusion de documents scientifiques de niveau recherche, publiés ou non, émanant des établissements d'enseignement et de recherche français ou étrangers, des laboratoires publics ou privés.

Theoretical calculations of excited rovibrational levels of HD. Term values and transition probabilities of VUV electronic bands[★]

H. Abgrall and E. Roueff

Laboratoire Univers et Théorie, UMR 8102 du CNRS, Observatoire de Paris, Section de Meudon, Place Jules Janssen, 92195 Meudon, France
e-mail: EveLyne.Roueff@obspm.fr

Received 24 June 2005 / Accepted 12 July 2005

ABSTRACT

In this paper, we derive the theoretical properties of rovibrational levels belonging to excited B, C, B', and D electronic states of HD. We compute the eigenvalues and eigenfunctions of the nuclear coupled Schroedinger equations using ab initio electronic molecular properties available in the literature. Transition wavenumbers and spontaneous emission probabilities are calculated for all transitions belonging to B–X, C–X, B'–X, and D–X electronic band systems of HD when the upper rotational quantum number is below or equal to 10. We compare our results with available experimental values: the accuracy in the wavenumbers is on the order of 3 reciprocal centimetres, whereas the intensity properties are satisfactorily reproduced. The origin of the remaining discrepancies is analyzed.

Key words. molecular processes – molecular data – line: identification – radiation mechanisms: general

1. Introduction

HD is the simplest 2-electron system to consider after H₂. There have been few spectroscopic studies of this molecule since the VUV absorption analysis of HD by Dabrowski & Herzberg (1976) that followed the study by Monfils (1965). Ubachs and colleagues (de Lange et al. 2000; Hinnen et al. 1995; Reinhold et al. 1999) have performed specific experimental studies at very short wavelengths and discussed the nonadiabatic coupling effects in the Rydberg excited electronic levels of HD. Symmetry-breaking effects between *u* and *g* electronic excited levels have been inferred from these experiments. On the other hand, HD has been detected in VUV absorption in diffuse and translucent clouds thanks to the Copernicus mission (Wright & Morton 1979) and FUSE (Far Ultra-violet Spectroscopic Explorer), both in galactic and extragalactic environments (André et al. 2004; Lacour et al. 2005). The derivation of comprehensive column densities of HD requires precise knowledge of the absorption oscillator strengths or emission transition probabilities.

These observations motivated us to undertake systematic calculations of the electronic spectrum of HD using the same approach that we used for H₂ (Abgrall et al. 1993, 1994, 1999, 2000). These results extend the systematic calculations by Allison & Dalgarno (1969) in a one-dimensional approximation for the excited and ground electronic states involved

in the Lyman (B–X) and Werner (C–X) band systems, without considering centrifugal barrier effects. The theoretical aspects are summarized in Sect. 2, including the derivation of the coupled Schroedinger equations and the molecular data required to derive the wavefunctions and matrix elements of the dipole transition moments. We report our results of transition wavenumbers, emission transition probabilities, and total radiative lifetimes in Sect. 3. Comparison of our calculations of both transition wavenumbers and intensities and the available experimental results is discussed in Sect. 4, and the summary of our results given in Sect. 5.

2. Theoretical context

We consider the transitions between the upper B (¹Σ_u), C (¹Π_u), B' (¹Σ_u), D (¹Π_u) electronic rovibrational levels and those corresponding to the ground electronic states of HD. The ground X ¹Σ_g⁺ electronic state is isolated from the other excited electronic state, so the different rotational and vibrational eigenfunctions and their eigenvalues are obtained by solving the one dimensional Schroedinger equation without introducing any coupling. The repulsive centrifugal barrier potential is introduced in addition to the ground electronic potential computed by Wolniewicz (1993) including relativistic and adiabatic corrections for H₂ and introducing the reduced mass of HD, $\mu = 1223.8988$ a.u. according to Senn et al. (1988).

2.1. General considerations

The rovibronic upper states are obtained by including the non-adiabatic couplings between the four B, B', C, and

[★] Electronic data tables of excited states properties (full Tables 5–10) and transition probabilities (full Tables 11–16) are only available at the CDS via anonymous ftp to cdsarc.u-strasbg.fr (130.79.128.5) or via <http://cdsweb.u-strasbg.fr/cgi-bin/qcat?J/A+A/445/361>

D excited electronic states. We expand the total electronic and nuclear wave function Φ_{SvJ} characterized by the electronic S label, the total parity $(+,-)$, and the vibrational v and rotational J nuclear quantum numbers over the electronic Born-Oppenheimer (B.O.) wavefunctions corresponding to a single electronic state:

$$\Phi_{SvJ}^{+/-} = \sum_T \Psi_{TJ} \times f_{STvJ}. \quad (1)$$

Each Ψ wave function is the product of the electronic B.O. wavefunction, corresponding to a particular electronic state referred by T index, and the pure rotational nuclear wavefunction. When the electronic state has a Σ^+ symmetry, the parity of the total wave function is given by the parity of J (e levels). In the case of doubly degenerate Π electronic states, no definite parity holds. However, non-adiabatic coupling between different electronic states may split the electronic potential curves according to the parity. For example, levels belonging to C^+ and D^+ have a parity given by $(-1)^J$ and labelled e -levels, whereas levels belonging to C^- and D^- have a parity given by $(-1)^{J+1}$ and labelled f -levels.

We calculate the rovibrational wave functions f_{STvJ} and the corresponding energy levels E_{vJ} by searching the eigenvalues of the coupled equations (split according to their total parity and total angular momentum J), obtained when writing the Schrodinger equation of the total wave function as described by Senn et al. (1988). The diagonal terms are given by the adiabatic electronic potentials, and the off-diagonal terms are rotational (Σ - Π) and radial (Σ - Σ or Π - Π) electronic coupling matrix elements.

HD is not a homonuclear molecule, whereas inversion symmetry applies for pure B.O. electronic states. Then, gerade and ungerade labels are not completely exact good quantum numbers for the rovibronic states. Indeed, very faint electric dipole transitions between so-called g electronic levels (as EF-X, GK-X, etc.) have been observed (see for example Dabrowski & Herzberg 1976; Hinnen et al. 1995), whereas they are completely forbidden if inversion symmetry holds. However, the rovibrational coupling between the u and g B.O. states is very weak for the majority of states, so we neglect it in our calculations. The lack of accuracy resulting from this assumption will be discussed when we compare our results with experimental data. We introduce the weight of each T electronic state in the expansion of the rovibrational wave function:

$$\rho(T) = \int (f_{STvJ}(R))^2 dR. \quad (2)$$

The normalization is such that $\rho(B) + \rho(C) + \rho(B') + \rho(D) = 1$. Except for very specific cases, one value of T is preponderant, which allows us to define an electronic label S for the total wave function that, by convention, corresponds to the state of greatest weight. The spontaneous emission probability or Einstein A coefficient, expressed in s^{-1} , is given by the expression:

$$A(v_j, v_i; J_j, J_i) = \frac{1}{4\pi\epsilon_0} \frac{4}{3\hbar^4 c^3 (2J_j + 1)} (E_{v_j J_j} - E_{v_i J_i})^3 |M_{S\alpha}|^2 \quad (3)$$

E_{vJ} is the energy of the level (v, J) , $M_{S\alpha}$, the electric transition dipole matrix element between wavefunctions of excited

$S(v_j, J_j)$, and ground electronic $X(v_i, J_i)$ states, while α indicates whether the spectroscopic branch label is P, Q, or R corresponding to $\Delta J = -1, 0, 1$, respectively. When the emission takes place in the X continuum states, the expression is modified in order to account for the energy normalization of the continuum wave function:

$$A(v_j, e_i; J_j, J_i) = \frac{1}{4\pi\epsilon_0} \frac{4}{3\hbar^4 c^3 (2J_j + 1)} (E_{v_j J_j} - E_{e_i J_i})^3 |M_{S\alpha}|^2. \quad (4)$$

The continuum index of the kinetic energy of dissociating atoms e_i replaces the vibrational label v_i . The total emission probability, which produces dissociation from one specific excited level $(v_j; J_j)$, is obtained by performing the integration of the emission probability over all possible kinetic energies and by summing over the different rotational quantum numbers of the lower states with appropriate selection rules:

$$A_c(v_j; J_j) = \sum_{J_i} \int_0^\infty A(v_j, e_i; J_j, J_i) de_i. \quad (5)$$

The radiative lifetime of one specific excited $(v_j; J_j)$ level is given by the inverse of the total emission probability $A_t(v_j; J_j)$ which is expressed as:

$$A_t(v_j; J_j) = A_c(v_j; J_j) + \sum_{v_i, J_i} A(v_j, v_i; J_j, J_i). \quad (6)$$

The transition dipole matrix elements $M_{S\alpha}$ appearing in Eq. (2) are given by the following expressions:

$$M_{SP} = (J_j + 1)^{1/2} \{ \langle f_{Bv_j J_j} | M_{BX} | f_{Xv_i J_i} \rangle + \langle f_{B'v_j J_j} | M_{B'X} | f_{Xv_i J_i} \rangle + J_j^{1/2} \{ \langle f_{C^+v_j J_j} | M_{CX} | f_{Xv_i J_i} \rangle + \langle f_{D^+v_j J_j} | M_{DX} | f_{Xv_i J_i} \rangle \} \} \quad (7)$$

$$M_{SQ} = (2J_j + 1)^{1/2} \{ \langle f_{C^-v_j J_j} | M_{CX} | f_{Xv_i J_i} \rangle + \langle f_{D^-v_j J_j} | M_{DX} | f_{Xv_i J_i} \rangle \} \quad (8)$$

$$M_{SR} = J_j^{1/2} \{ \langle f_{Bv_j J_j} | M_{BX} | f_{Xv_i J_i} \rangle + \langle f_{B'v_j J_j} | M_{B'X} | f_{Xv_i J_i} \rangle - (J_j + 1)^{1/2} \{ \langle f_{C^+v_j J_j} | M_{CX} | f_{Xv_i J_i} \rangle + \langle f_{D^+v_j J_j} | M_{DX} | f_{Xv_i J_i} \rangle \} \} \quad (9)$$

where M_{BX} , M_{CX} , $M_{B'X}$, and M_{DX} are the real values of the electronic transition moments calculated for each internuclear distance in the B.O. approximation, and P, Q, R refer to the different branches of the transitions. We see that the P and R branches connect e -levels belonging to B, B', C⁺, and D⁺ electronic states, whereas Q branches connect f -levels involving C⁻ and D⁻ electronic states.

The absorption oscillator strengths can be derived from the spontaneous emission probabilities via the following expressions:

$$f(v_i, v_j; J_i, J_j) = \frac{4\pi\epsilon_0}{e^2} \frac{m_e c}{8\pi^2 \sigma^2} \frac{(2J_j + 1)}{2J_i + 1} A(v_j, v_i; J_j, J_i) \quad (10)$$

where m_e is the electron mass, σ the wavenumber of the transition. This expression has a very convenient numerical value when σ is expressed in reciprocal centimetres:

$$f(v_i, v_j; J_i, J_j) = 1.49919 \frac{1}{\sigma^2} \frac{(2J_j + 1)}{2J_i + 1} A(v_j, v_i; J_j, J_i). \quad (11)$$

Table 1. Molecular ab initio properties used in the calculations.

Quantity	Reference
X $^1\Sigma_g^+$ adiabatic potential	Wolniewicz (1993)
B $^1\Sigma_u^+$ adiabatic potential	Staszewska & Wolniewicz (2002)
B' $^1\Sigma_u^+$ adiabatic potential	Staszewska & Wolniewicz (2002)
C $^1\Pi_u$ adiabatic potential	Wolniewicz & Staszewska (2003b)
D $^1\Pi_u$ adiabatic potential	Wolniewicz & Staszewska (2003b)
Off-diagonal rotational and radial matrix elements	Wolniewicz & Dressler (1988)
B–X transition moment	Wolniewicz & Staszewska (2003a)
B'–X transition moment	Wolniewicz & Staszewska (2003a)

2.2. Numerical method and molecular properties

The integrations are performed by using atomic units (the atomic unit of energy is $219474.631 \text{ cm}^{-1}$ from the latest definitions). We solve the nuclear coupled equations by using the Numerov method as described by Johnson (1978), similarly to our previous calculations of H_2 or D_2 . We take an integration step length of 0.01 au, an outer integration limit of 30 au, and use a spline interpolation to calculate the electronic matrix elements at the integration grid points. In the absence of g – u coupling, the dissociating limits of the B, C, and B' states corresponding to $\text{H}(1s)+\text{D}(2s, 2p)$ or $\text{D}(1s)+\text{H}(2s, 2p)$ are not distinguished. The values labelled $D_{(2)}$, relative to the ground state of the neutral molecules, X $^1\Sigma_g^+$ ($v = 0, J = 0$) are adopted from Table IX of Dressler & Wolniewicz (1986). The dissociation limit of the D state involves $n = 3$ of H or D and is labelled $D_{(3)}$. We take the theoretical value derived from the adiabatic approximation (Senn et al. 1988). The corresponding values are $D_{(2)} = 118\,676.087 \text{ cm}^{-1}$ and $D_{(3)} = 133\,911.154 \text{ cm}^{-1}$. The ab initio data used in our calculations are displayed in Table 1.

When considering the non-adiabatic effects within the four excited states for which the coupling is most important, we expect that the accuracy is several reciprocal centimeters, due to the neglect of the other weakly coupled states combined with the uncertainties involved in the ab initio data themselves. Our former calculations on H_2 and D_2 transition wavenumbers (Abgrall et al. 1993, 1994, 1999) were closer to the experimental rovibronic levels up to the higher J , as we were able to make slight adjustments of the diagonal potential data for the unperturbed levels involved ($J = 0$ or $J = 1$). The discrepancy in the energy terms was less than 1 cm^{-1} , even for the higher rotational levels. The transition probability is less sensitive to the molecular potentials, except for the few perturbed levels where the energy difference between adiabatic values is critical.

We were not able to use this semi-empirical procedure in the case of HD, since there are not enough published experimental levels for $J = 0$ or $J = 1$ and because the g – u coupling induces shifts in a random way in the rovibrational level energy values (see discussion in Sect. 4.1.2 and lower part of Fig. 1). The recent ab initio data used in the present work are given for a large number of internuclear distances and are much more accurate than the values used in our previous calculations of H_2 and D_2 .

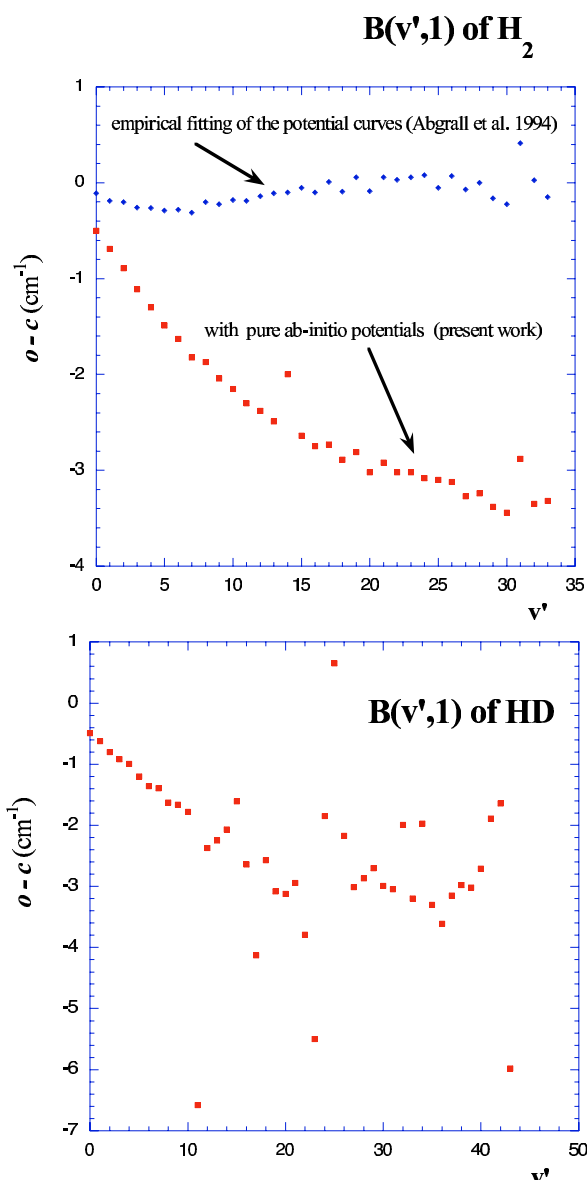


Fig. 1. Upper plot: o–c of H_2 versus v' for the levels $B(v', 1)$. Lower plot: o–c of HD versus v' for the levels $B(v', 1)$.

3. Results

We have solved the nuclear coupled Schroedinger equations up to $J = 10$ and obtained the corresponding discrete

eigenfunctions and eigenvalues for the excited electronic states B, C, B' and D below the dissociation limit $D_{(2)}$ in the non-adiabatic approximation. As the D long range potential converges towards the H(3p) or D(3p) state, discrete levels belonging to D may occur between $D_{(2)}$ and $D_{(3)}$. In the case of H₂ and D₂, the e levels belonging to D⁺ are strongly predissociated by B' ($u-u$ rotational coupling), and only f -levels belonging to D⁻ are seen in emission. This does not hold for HD, as $g-u$ coupling takes place between f -levels belonging to D $^1\Pi_u^-$ and I $^1\Pi_g^-$ (Dehmer & Chupka 1983). However, as we neglect the $g-u$ coupling, we also calculate the Q branches corresponding to D⁻ – X transitions for excited level energies between $D_{(2)}$ and $D_{(3)}$ in the adiabatic approximation.

Neglecting non-adiabatic corrections for the X lower rovibrational levels may also produce up to a 5 cm⁻¹ discrepancy in the energy terms when compared to experimental values (Wolniewicz 1993, 1995). So, as in our previous work on H₂ and D₂, we introduce, if available, the experimental energy levels (Dabrowski & Herzberg 1976) corresponding to the electronic X ground state to derive the transition energies involved in the various electronic bands. Thus, the accuracy of the transition wavenumbers reported here depends only on the uncertainties involved in the calculations of excited level energies.

3.1. Excited level properties: energy terms, electronic weight factors, total radiative decay probability, radiative dissociation probability

Tables 5–10 give the presently calculated rovibrational energy terms obtained with the origin at the rovibrational ground level $v = 0, J = 0$ of the X electronic state, the total spontaneous emission probabilities $A_i(v_j; J_j)$, and the emission probability towards the continuum $A_c(v_j; J_j)$ expressed in s⁻¹ as described in Eqs. (3)–(5) for the different excited levels included, i.e. B, C, B', and D for rotational quantum number values from 0 to 10. The tables also include the electronic weight factors $\rho(B), \rho(C), \rho(B'), \rho(D)$ of the B.O. states for each rovibrational level of definitive parity, as defined in Sect. 2. Tables 5–8 present the e manifold which involves only P and R branches in radiative transitions with the ground electronic state. When $J > 0$, we include the coupling between the four B, C⁺, B', D⁺ states that incorporate both a significant rotational coupling between Σ and Π states and a weak radial coupling between $\Sigma-\Sigma$, on the one hand and $\Pi-\Pi$, on the other. The rotational coupling does not occur when $J = 0$, as the Π levels have no rotational quantum number below 1, and rovibrational levels with $J = 0$ belonging to B and B' are coupled by the corresponding weak radial coupling. Tables 9–10 present the f manifold that involves only Q branches in radiative transitions with the ground electronic state. The C⁻ and D⁻ are coupled by a weak non-adiabatic $u-u$ radial coupling. Above the energy corresponding to $D_{(2)}$, the calculations are only performed in the adiabatic approximation in a single potential approach, as stated before.

We display in Table 2 an example of the data given in Tables 5–10 for the states with a rotational quantum number $J = 1$ belonging mainly to B. These levels are attained in absorption from the electronic ground state via the R(0)

transitions of the Lyman band system and can only be perturbed by levels of e parity. One value of ρ is dominant (corresponding to state B in Table 2), which is also true in most cases, and justifies using the classification B, C, B' or D and labelling the levels with the name of the B.O. state of greatest electronic weight factor, ρ . It may, however, happen that one value of ρ becomes close to 0.5 for a specific rovibrational level, in which case the classification in terms of B.O. states becomes arbitrary. It is thus necessary to include an extra label, noted ν , to give the order of the level in ascending energies within a given parity (e or f) starting from $\nu = 1$. In the example reported in Table 2, the $B \nu = 9, J = 1$ level energy is not directly after the $B, \nu = 8, J = 1$ level. We also notice that the probability of dissociating into the continuum increases with the energy term values, and the photodissociation probability (ratio between the probability to fluorescence towards the continuum and the total emission probability) is almost 1 for the higher terms so that the corresponding levels are not seen in spectroscopic experiments.

3.2. Tables of transitions and line emission probabilities

Emission transition probabilities are displayed in Tables 11–16 for excited rotational quantum numbers less than 11. We also indicate, when available, the discrepancies with the experimental determinations. The labels (mn) of the last column indicate how the transition wavenumbers have been derived:

- $m = 1$ if the X energy terms are taken from experiments (Dabrowski & Herzberg 1976);
- $m = 2$ if the X energy terms are theoretical values from Wolniewicz (1995);
- $m = 3$ if we use our own calculations in the absence of any other information;
- $n = 0$ indicates that no experimental information is available for the transition;
- $n = 1$ corresponds to the transition wavenumber given by Dabrowski & Herzberg (1976);
- $n = 2$ corresponds to the experimental values of Dehmer & Chupka (1983);
- $n = 3$ corresponds to the experimental values of Takezawa & Yanaka (1972);
- $n = 4$ corresponds to the experimental values of Monfils (1965).

4. Comparison with experiments and discussion

4.1. Experimental transition wavenumbers

A few transition energies have been derived recently by Hinnen et al. (1995) in the region between 102 040 cm⁻¹ and 108 700 cm⁻¹ with a claimed accuracy of 0.035 cm⁻¹. We collect the corresponding values in Table 3 and compare our calculated values with those of Dabrowski & Herzberg (1976) and those of Hinnen et al. (1995). The discrepancies in the B levels are usually less than 3 cm⁻¹ and less than 1 cm⁻¹ for C states.

In Tables 3, 11 to 16, o–c (observed–calculated) is generally negative and goes from about –0.5 cm⁻¹ to about –5 cm⁻¹.

Table 2. Properties of the v' , $J = 1$ levels belonging to the B $^1\Sigma_u$ electronic state. See text for explanations of the various columns.

v	v'	J	ρ (B)	ρ (C ⁺)	ρ (B')	ρ (D ⁺)	T cm ⁻¹	A_t s ⁻¹	A_c s ⁻¹
0	1	1	1.000E+00	1.360E-05	4.380E-06	1.420E-07	90 429.52	1.870E+09	4.320E-01
1	2	1	1.000E+00	2.000E-05	1.110E-05	1.360E-07	91 575.73	1.760E+09	3.678E+01
2	3	1	1.000E+00	2.660E-05	1.700E-05	1.310E-07	92 693.83	1.670E+09	5.761E+02
3	4	1	1.000E+00	3.460E-05	2.210E-05	1.270E-07	93 785.45	1.580E+09	4.471E+04
4	5	1	1.000E+00	4.170E-05	2.660E-05	1.230E-07	94 851.46	1.500E+09	2.010E+05
5	6	1	1.000E+00	5.050E-05	3.050E-05	1.190E-07	95 892.41	1.430E+09	3.403E+06
6	7	1	1.000E+00	6.250E-05	3.410E-05	1.150E-07	96 908.71	1.360E+09	2.203E+07
7	8	1	1.000E+00	8.110E-05	3.720E-05	1.120E-07	97 900.66	1.300E+09	4.576E+07
8	9	1	1.000E+00	1.940E-04	3.990E-05	1.110E-07	98 868.56	1.250E+09	2.562E+08
9	11	1	1.000E+00	1.370E-04	4.240E-05	1.050E-07	99 812.80	1.190E+09	3.094E+08
10	12	1	1.000E+00	2.480E-04	4.460E-05	1.070E-07	100 733.51	1.140E+09	4.617E+08
11	14	1	1.000E+00	3.470E-04	4.650E-05	9.610E-08	101 631.30	1.100E+09	4.400E+08
12	15	1	1.000E+00	2.650E-04	4.810E-05	1.050E-07	102 506.03	1.060E+09	4.219E+08
13	17	1	9.980E-01	2.090E-03	4.960E-05	9.190E-08	103 358.80	1.020E+09	5.171E+08
14	18	1	1.000E+00	2.810E-04	5.070E-05	9.700E-08	104 188.72	9.800E+08	4.910E+08
15	19	1	8.790E-01	1.210E-01	4.450E-05	1.200E-06	104 994.20	9.660E+08	4.318E+08
16	21	1	1.000E+00	2.970E-04	5.260E-05	8.680E-08	105 784.26	9.120E+08	4.925E+08
17	22	1	9.970E-01	2.680E-03	5.290E-05	1.300E-07	106 549.75	8.810E+08	4.784E+08
18	24	1	9.990E-01	4.010E-04	5.370E-05	1.040E-07	107 295.36	8.510E+08	4.936E+08
19	25	1	9.990E-01	1.030E-03	5.390E-05	1.030E-07	108 019.75	8.240E+08	4.878E+08
20	27	1	9.990E-01	6.990E-04	5.430E-05	1.030E-07	108 724.69	7.980E+08	4.780E+08
21	28	1	9.990E-01	6.630E-04	5.430E-05	1.000E-07	109 409.11	7.730E+08	4.669E+08
22	30	1	9.980E-01	2.090E-03	5.440E-05	1.100E-07	110 074.80	7.510E+08	4.559E+08
23	32	1	9.990E-01	5.330E-04	5.410E-05	1.420E-07	110 720.25	7.290E+08	4.520E+08
24	34	1	9.700E-01	2.990E-02	5.320E-05	3.610E-07	111 348.77	7.200E+08	4.385E+08
25	35	1	9.990E-01	5.020E-04	5.350E-05	1.130E-07	111 955.15	6.900E+08	4.499E+08
26	37	1	9.860E-01	1.370E-02	5.180E-05	2.840E-07	112 543.42	6.770E+08	4.455E+08
27	40	1	9.990E-01	5.660E-04	5.240E-05	7.590E-08	113 115.19	6.570E+08	4.454E+08
28	41	1	9.970E-01	2.750E-03	5.130E-05	1.270E-07	113 666.81	6.430E+08	4.417E+08
29	44	1	9.990E-01	7.750E-04	5.080E-05	6.040E-08	114 200.75	6.300E+08	4.372E+08
30	45	1	9.980E-01	1.440E-03	4.960E-05	9.510E-08	114 714.88	6.180E+08	4.332E+08
31	48	1	9.990E-01	1.230E-03	4.880E-05	6.550E-08	115 210.55	6.090E+08	4.324E+08
32	50	1	9.990E-01	1.070E-03	4.710E-05	7.270E-08	115 685.51	6.020E+08	4.334E+08
33	52	1	9.980E-01	2.000E-03	4.590E-05	6.120E-08	116 140.46	5.970E+08	4.400E+08
34	54	1	9.990E-01	9.630E-04	4.420E-05	6.350E-08	116 572.39	5.940E+08	4.479E+08
35	57	1	9.970E-01	2.790E-03	4.320E-05	5.560E-08	116 980.94	5.970E+08	4.633E+08
36	58	1	9.990E-01	9.810E-04	4.380E-05	4.800E-08	117 361.52	6.020E+08	4.792E+08
37	61	1	9.970E-01	2.860E-03	5.250E-05	4.620E-08	117 711.40	6.160E+08	5.100E+08
38	62	1	9.990E-01	1.060E-03	9.700E-05	3.970E-08	118 022.62	6.370E+08	5.465E+08
39	65	1	9.970E-01	2.700E-03	3.450E-04	3.630E-08	118 286.74	6.860E+08	6.147E+08
40	67	1	9.970E-01	7.450E-04	2.040E-03	8.100E-08	118 487.95	7.860E+08	7.373E+08
41	70	1	9.660E-01	1.500E-02	1.820E-02	9.700E-04	118 607.05	9.650E+08	9.380E+08
42	73	1	9.870E-01	1.640E-03	1.110E-02	2.840E-06	118 650.59	1.100E+09	1.092E+09
43	75	1	9.590E-01	4.550E-04	4.030E-02	1.380E-04	118 667.59	1.090E+09	1.086E+09

Table 3. Comparison of present calculations of the transition wavenumbers of B–X, C⁺–X, and C[−]–X electronic band systems of HD with the high-resolution experimental determinations of Hinnen et al. (1995) (o₁–c) and Dabrowski & Herzberg (1976) (o₂–c).

Band system	v'	J'	v''	J''	σ (cm ^{−1})	o ₁ –c (cm ^{−1})	o ₂ –c (cm ^{−1})
B–X	12	0	0	1	102 397.35	−2.48	−1.99
	12	1	0	0	102 506.03	−2.47	−3.13
	12	1	0	2	102 238.91	−2.39	−2.11
	12	2	0	1	102 455.64	−2.57	−2.17
	12	2	0	3	102 012.55	−2.70	−2.40
	12	3	0	2	102 335.82	−2.96	−2.66
	13	0	0	1	103 250.31	−2.32	−2.01
	13	1	0	0	103 358.80	−2.76	−2.62
	13	1	0	2	103 091.68	−2.37	−1.82
	13	2	0	1	103 308.38	−2.41	−2.12
	13	2	0	3	102 865.29	−2.50	−2.15
	13	3	0	2	103 192.07	−0.42	−0.45
	13	3	0	4	102 575.89	−0.42	−0.33
	13	4	0	3	102 987.85	−2.75	−2.71
	13	4	0	5	102 202.72	−2.60	−2.76
	13	5	0	4	102 733.46	−7.79	−7.51
	13	6	0	5	102 410.93	−1.62	−1.72
	14	0	0	1	104 081.13	−2.39	−2.36
	14	1	0	0	104 188.72	−2.43	−2.24
	14	1	0	2	103 921.60	−2.40	−1.99
	14	2	0	1	104 136.13	−2.52	−2.48
	14	2	0	3	103 693.04	−2.47	−2.21
	14	3	0	2	104 013.05	−2.50	−2.33
	14	3	0	4	103 396.87	−2.44	−2.34
	14	4	0	3	103 820.63	−2.67	−2.54
	14	4	0	5	103 035.50	−2.66	−2.37
	14	5	0	4	103 560.13	−3.09	−2.85
	16	0	0	1	105 677.68	−2.55	−2.71
	16	1	0	0	105 784.26	−2.53	−2.72
	16	1	0	2	105 517.14	−2.47	−2.44
	16	2	0	1	105 729.66	−2.54	−1.77
	16	2	0	3	105 286.57	−2.51	−2.31
	16	3	0	2	105 603.59	−2.47	−3.06
	16	4	0	3	105 407.25	−2.59	−2.45
	17	0	0	1	106 444.10	−3.79	−3.94
	17	1	0	0	106 549.74	−3.59	−4.06
	17	1	0	2	106 282.62	−3.58	−4.08
	17	2	0	1	106 493.55	−3.44	−2.61
	17	2	0	3	106 050.46	−3.41	–
	17	3	0	2	106 365.41	−3.22	−3.40
	17	3	0	4	105 749.23	−3.14	−3.48
	17	4	0	3	106 166.55	−4.25	−3.62
	18	0	0	1	107 189.71	−2.33	−2.55
	18	1	0	0	107 295.36	−2.35	−2.55
	18	1	0	2	107 028.24	−2.30	−2.47
	18	2	0	1	107 238.92	−2.36	−2.58
	18	2	0	3	106 795.83	−2.33	−2.61
	18	3	0	2	107 110.15	−2.24	−2.49
	18	3	0	4	106 493.97	−2.27	−3.03
	18	4	0	3	106 910.37	−2.23	−2.52
	18	5	0	4	106 641.37	−0.17	−0.32
	18	6	0	5	106 307.99	−1.99	−2.65

The shift is only due to the uncertainty in the excited rovibrational levels. This discrepancy is, however, higher and irregular

Table 3. continued.

Band system	v'	J'	v''	J''	σ (cm ^{−1})	o ₁ –c (cm ^{−1})	o ₂ –c (cm ^{−1})
	19	0	0	1	107 914.87	−2.50	−3.04
	19	1	0	0	108 019.75	−2.52	−3.10
	19	1	0	2	107 752.63	−2.44	−2.94
	19	2	0	1	107 961.85	−2.49	−2.96
	19	2	0	3	107 518.76	−2.56	−2.96
	19	3	0	2	107 830.98	−2.45	−2.93
	19	3	0	4	107 214.80	−2.43	−2.80
	19	4	0	3	107 628.38	−2.53	−2.98
	19	5	0	4	107 355.37	−2.34	−2.85
C ⁺ –X	2	1	0	0	103 202.63	−0.55	−0.50
	2	1	0	2	102 935.51	−0.65	−0.83
	2	2	0	1	103 197.39	−0.57	−1.44
	2	2	0	3	102 754.30	−0.71	−0.32
	2	3	0	2	103 141.13	−0.85	−0.53
	2	3	0	4	102 524.95	−0.80	−0.73
	2	4	0	3	103 057.40	−0.76	−0.71
	2	4	0	5	102 272.27	−0.61	−0.56
	2	5	0	4	102 910.03	−0.58	0.05
	2	5	0	6	101 960.78	−0.02	−0.38
	2	6	0	5	102 720.33	−0.55	−0.52
	2	7	0	6	102 486.54	−0.25	−0.39
	4	1	0	0	106 732.53	−0.95	−0.94
	4	1	0	2	106 465.41	−0.90	−1.26
	4	2	0	1	106 720.87	−0.95	−1.03
	4	2	0	3	106 277.78	−0.95	−1.03
	4	3	0	2	106 658.13	−0.92	−0.95
	4	3	0	4	106 041.95	−0.85	−0.53
	4	4	0	3	106 544.56	−0.98	−1.13
	4	4	0	5	105 759.43	−0.88	−1.21
	4	5	0	4	106 380.08	−0.90	−1.16
	4	6	0	5	106 163.43	−0.01	−0.50
	5	4	0	5	107 357.78	−0.90	−1.06
	5	5	0	4	107 963.09	−1.22	−1.98
C [−] –X	2	1	0	1	103 112.91	−0.57	−1.17
	2	2	0	2	103 018.50	−0.65	0.22
	2	3	0	3	102 877.89	−0.72	−0.57
	2	4	0	4	102 691.86	−0.53	−0.36
	2	5	0	5	102 462.06	−0.52	−0.37
	2	6	0	6	102 189.52	−0.07	−0.40
	4	1	0	1	106 642.14	−0.94	−1.09
	4	2	0	2	106 539.88	−0.90	−1.00
	4	3	0	3	106 387.52	−0.96	−1.00
	4	4	0	4	106 185.90	−0.75	−1.21
	4	5	0	5	105 936.72	−0.78	−1.19
	5	4	0	4	107 787.23	−0.83	−1.40

for some specific cases. Four main sources can be invoked for these differences:

1. the ab initio electronic matrix elements are not accurate enough or the number of coupled u electronic states should be increased to more states;
2. the coupling between u and g states is neglected, so the corresponding approximation fails;

3. the transition labelling of Dabrowski & Herzberg (1976) is different from ours;
4. there are misprints in the data of Dabrowski & Herzberg (1976).

frequent, as shown in Table 4, and the 2-state approximation is usually not valid.

The corresponding examples are given below.

4.1.1. Discrepancies due to rotational or radial coupling between u states

We test the effect of the couplings by performing equivalent calculations but including H_2 parameters. In the upper part of Fig. 1, we display the $o-c$ values of H_2 taken from experimental determinations of Abgrall et al. (1993) and concerning the energy terms of $B(v', 1)$ versus the vibrational quantum numbers implied. We report both our previous results derived by semi-empirical fitting of the excited potential curves (Abgrall et al. 1994) and the results obtained by using pure ab initio data used for HD (cf. Table 1), but including the reduced mass of H_2 . We note first that the $o-c$ values reported from our previous work are within a 0.5 reciprocal centimetre. With pure ab initio data, there is a regular increase of $|o-c|$ from 0.5 to 3 cm^{-1} with the vibrational quantum number, as other excited electronic levels get close and may perturb the calculated term. This means that the expansion of the total wave function should include supplementary electronic states of u symmetry such as B'' , D' etc. However, two extra features appear for $v' = 14$ and 31. We infer from our previous studies that the perturbation of the $B(14, 1)$ level by the $C(3, 1)$ level is not fully calculated from ab initio calculations. An additional coupling has to be introduced to improve the calculation corresponding to $B(31, 1)$, where the coupling with B'' should be taken into account.

4.1.2. Discrepancies due to $g-u$ coupling

The lower part of Fig. 1 displays the $o-c$ values of the same $B(v', 1)$ transition wavenumbers for HD obtained in the present work without taking the $g-u$ coupling into account. The values are also negative and show a slight increase of $|o-c|$ up to $v' = 10$. For higher values of v' , the points are significantly random, and we tentatively explain the deviations as due to coupling with the $EF^1\Sigma_g^+$ electronic state. For example, in the case of $B(11, 1)$, $o-c = -6.5$ cm^{-1} , i.e. 4 cm^{-1} below the value obtained for $B(10, 1)$.

We display in Table 4 the different experimental terms corresponding to e parity levels reported in Dabrowski & Herzberg (1976) with a rotational quantum number $J = 1$ for any electronic band system. The $B(11, 1)$ term has been measured 8.76 cm^{-1} below the $EF(4, 1)$ term. We thus conclude that a significant perturbation occurs between these two levels. In order to evaluate the order of magnitude for this coupling, we use a two-state perturbation approximation and estimated the borrowing effect, which accounts for the emission probability of the EF state towards X . We find in this way that the emission probability lost by $B(11, 1)$ when we incorporate $g-u$ coupling is 4/8.76, i.e. about 40%. However, such coincidences are not

4.1.3. Discrepancies due to incorrect line assignments

The wavenumbers of the transitions $C-X$ (5–10) $R(5)$ and $C-X$ (5–0) $R(5)$ reported in Table 6 have -85.51 and -86.35 cm^{-1} differences, respectively, with Dabrowski & Herzberg (1976) data, whereas the wavenumbers of the $B-X$ (20–0) $R(5)$ transition reported in Table 2 display a difference of 81.55 cm^{-1} . The corresponding $o-c$ values become -2.92 , -2.09 , and -1.88 cm^{-1} if we exchange the assignments of $C(5, 6)$ and $B(20, 6)$ levels. We may justify these assumptions by considering the electronic weight factors of the levels involved, i.e. $C(5, 6)$ and $B(20, 6)$. Indeed, $C(5, 6)$ has an electronic weight factor for state B of 0.269 and an electronic weight factor for state C of 0.731, whereas $B(20, 6)$ has an electronic weight factor for state B of 0.739 and an electronic weight factor for state C of 0.261. There is also a change of assignment between $C(4, 7)$ and $B(18, 7)$ levels, as well as between $C(11-5)$ and $B(33, 5)$ levels.

4.1.4. Other discrepancies

Some significant discrepancies between calculations and experiments are still present. We suspect a misprint for the $R(1)$, $R(2)$, $R(3)$ transitions belonging to the $B-X$ (9–8) band, because a change of the wave number of 2000 cm^{-1} in the Dabrowski & Herzberg (1976) values gives an $o-c$ value of -2.4 , -2.41 , -2.53 cm^{-1} , comparable to the other $o-c$ values involving B , $v = 9$ levels. The same conjecture applies for the $C-X$ (12–16) band concerning the P and Q transitions reported in Tables 6 and 9, respectively. An $o-c$ value of 153.73 cm^{-1} also occurs for the $B'-X$ (3–0) $R(5)$ in Table 7, for which no obvious explanation can be found.

4.2. Comparison with experimental intensities

Ajello et al. (2005) have recently measured the intensity of a fluorescence experimental spectrum at a 0.16 Å *FWHM* spectral resolution, obtained by exciting HD molecules at a temperature of 300 K, with a monoenergetic 100 eV electron beam. The aim of this experiment was the determination of the electronic excitation cross sections of HD by electrons through a comparison of experimental and simulated spectra using the calculations reported here.

As for H_2 (Liu et al. 2002) and D_2 (Abgrall et al. 1999), the most important path is the direct excitation in which the electrons excite HD via the electric-dipole transitions towards B , C , B' , and D states of u symmetry. The simulated and experimental spectra generally agree very satisfactorily when a direct excitation mechanism is invoked. The differences are discussed below and arise from an additional excitation process.

Table 4. Experimental term values of Dabrowski & Herzberg (1976) for $J = 1$ sorted in ascending order of energy.

T^a cm ⁻¹	ΔT^b cm ⁻¹	label	v	T^a cm ⁻¹	ΔT^b cm ⁻¹	label	v
90 429.10	–	B	0	110 167.49	96.42	EF	18
91 575.17	1146.07	B	1	110 671.61	504.12	B'	0
92 693.09	1117.92	B	2	110 714.81	43.20	B	23
93 784.58	1091.49	B	3	110 750.17	35.36	EF	19
94 850.53	1065.95	B	4	111 284.28	534.11	EF	20
95 891.27	1040.74	B	5	111 294.15	9.87	C ⁺	7
96 907.41	1016.14	B	6	111 346.98	52.83	B	24
97 899.33	991.92	B	7	111 901.91	554.93	G	0
98 866.99	967.66	B	8	111 938.96	37.05	EF	21
99 276.49	409.50	C ⁺	0	111 955.86	16.90	B	25
99 811.20	534.71	B	9	112 316.52	360.66	B'	1
100 627.57	816.37	EF	2	112 425.05	108.53	EF	22
100 731.79	104.22	B	10	112 541.31	116.26	B	26
101 289.69	557.90	C ⁺	1	112 621.45	80.14	C ⁺	8
101 624.78	335.09	B	11	113 112.24	490.79	B	27
101 633.54	8.76	EF	4	113 664.00	551.76	B	28
102 503.72	870.18	B	12	113 783.00	119.00	G	1
102 586.15	82.43	EF	5	113 842.67	59.67	B'	2
103 202.15	616.00	C ⁺	2	113 843.13	0.46	C ⁺	9
103 356.61	154.46	B	13	114 198.10	354.97	B	29
103 503.27	146.66	EF	7	114 711.95	513.85	B	30
104 186.71	683.44	B	14	114 959.75	247.80	C ⁺	10
104 340.24	153.53	EF	8	115 207.54	247.79	B	31
104 870.54	530.30	EF	9	115 237.65	30.11	B'	3
104 992.64	122.10	B	15	115 666.16	428.51	G	2
105 018.76	26.12	C ⁺	3	115 683.58	17.42	B	32
105 301.32	282.56	EF	10	115 963.81	280.23	C ⁺	11
105 781.68	480.36	B	16	116 137.32	173.51	B	33
105 979.49	197.81	EF	11	116 570.47	433.15	B	34
106 545.67	566.18	B	17	116 977.70	407.23	B	35
106 571.02	25.35	EF	12	117 357.97	380.27	B	36
106 731.75	160.73	C ⁺	4	117 540.00	182.03	G	3
107 142.65	410.90	EF	13	117 598.62	58.62	C ⁺	13
107 292.85	150.20	B	18	117 708.31	109.69	B	37
107 766.31	473.46	EF	14	118 019.70	311.39	B	38
108 016.73	250.42	B	19	118 199.45	179.75	C ⁺	14
108 349.90	333.17	C ⁺	5	118 283.78	84.33	B	39
108 382.64	32.74	EF	15	118 485.30	201.52	B	40
108 721.62	338.98	B	20	118 605.22	119.92	B	41
108 975.84	254.22	EF	16	118 624.21	18.99	C ⁺	15
109 406.23	430.39	B	21	118 649.01	24.80	B	42
109 568.85	162.62	EF	17	118 661.67	12.66	B	43
109 871.28	302.43	C ⁺	6	118 846.85	185.18	C ⁺	12
110 071.07	199.79	B	22				

^a Term values. ^b Difference between two successive term values.

4.2.1. Role of the cascades via E, F g states

In some wavenumber regions, experimental peaks are not reproduced by the calculations (see for example Fig. 4 of

Ajello et al. 2005). These peaks correspond to transitions emitted by the low vibrational levels of B ($v = 0-3$) and involve an indirect excitation mechanism via the so-called EF g electronic states. This mechanism has already been described for H₂

Table 5. Properties of B $^1\Sigma_u$ rovibrational states: electronic weight factors, term value, total spontaneous emission probability (s^{-1}) and total dissociation probability (s^{-1}). Full table available in electronic form at the CDS.

v	ν	J	$\rho(B)$	$\rho(C)$	$\rho(B')$	$\rho(D)$	T cm $^{-1}$	A_t s $^{-1}$	A_c s $^{-1}$
0	1	0	1.00E+00	0.00E+00	4.39E-06	0.0	90 400.17	1.88E+09	4.249E-01
1	2	0	1.00E+00	0.00E+00	1.12E-05	0.00E+00	91 547.68	1.76E+09	3.186E+01
2	3	0	1.00E+00	0.00E+00	1.70E-05	0.00E+00	92 666.88	1.67E+09	5.878E+02

Table 6. Properties of C $^+1\Pi_u$ rovibrational states: electronic weight factors, term value, total spontaneous emission probability (s^{-1}) and total dissociation probability (s^{-1}). Full table available in electronic form at the CDS.

v	ν	J	$\rho(B)$	$\rho(C)$	$\rho(B')$	$\rho(D)$	T cm $^{-1}$	A_t s $^{-1}$	A_c s $^{-1}$
0	10	1	2.87E-04	1.00E+00	2.14E-06	1.2E-06	99 276.56	1.18E+09	5.121E+04
1	13	1	5.78E-04	9.99E-01	2.19E-06	4.0E-06	101 290.22	1.16E+09	2.169E+05
2	16	1	2.36E-03	9.98E-01	2.21E-06	6.2E-06	103 202.63	1.15E+09	1.254E+06

Table 7. Properties of B' $^1\Sigma_u$ rovibrational states: electronic weight factors, term value, total spontaneous emission probability (s^{-1}) and total dissociation probability (s^{-1}). Full table available in electronic form at the CDS.

v	ν	J	$\rho(B)$	$\rho(C)$	$\rho(B')$	$\rho(D)$	T cm $^{-1}$	A_t s $^{-1}$	A_c s $^{-1}$
0	24	0	1.03E-05	0.00E+00	1.00E+00	0.00E+00	110 633.49	3.76E+08	5.79E-01
1	28	0	2.39E-05	0.00E+00	1.00E+00	0.00E+00	112 284.12	3.26E+08	5.281E-01
2	32	0	3.34E-05	0.00E+00	1.00E+00	0.00E+00	113 813.92	2.78E+08	2.808E+00

Table 8. Properties of D $^+1\Pi_u$ rovibrational states: electronic weight factors, term value, total spontaneous emission probability (s^{-1}) and total dissociation probability (s^{-1}). Full table available in electronic form at the CDS.

v	ν	J	$\rho(B)$	$\rho(C)$	$\rho(B')$	$\rho(D)$	T cm $^{-1}$	A_t s $^{-1}$	A_c s $^{-1}$
0	39	1	3.42E-07	2.03E-06	1.76E-03	9.98E-01	113 066.22	3.56E+08	9.68E-01
1	47	1	3.27E-07	7.87E-06	6.58E-03	9.93E-01	115 006.28	3.50E+08	1.69E+00
2	56	1	2.26E-06	4.50E-04	4.75E-03	9.95E-01	116 852.19	3.45E+08	1.93E+04

(Liu et al. 2002, 2003) and D₂ (Abgrall et al. 1999). In addition, as discussed in Ajello et al. (2005), the EF states are perturbed by some states of u character and may thus be excited by electrons via allowed electric dipole transitions. Then the EF levels fluoresce mainly towards B ($v = 0-3$) levels via infrared emission, which finally emit UV photons towards the X electronic ground state. Figure 4 in Ajello et al. (2005), displays examples of such features, which are reproduced when the excitation in the EF states is taken into account (Fig. 5 of the same paper). A detailed description of this treatment will be reported in a future paper.

4.2.2. Direct de-excitation from E, F g states

We do not systematically calculate the direct de-excitation from EF, GK, towards X, as comparison with experiments shows that the corresponding effect is weak at the resolution in Ajello et al. (2005). However we do notice some rare features where the calculated intensity is above the experimental value, which may be explained by the borrowing effect described in Sect. 4.1.2. We discuss here the feature at 1333 Å displayed in Fig. 2e of Ajello et al. (2005). The 1333.24054 Å wavelength corresponds to

the B–X (11–9) P(2) transition (Table 5 and Dabrowski & Herzberg 1976). However, there is a close transition belonging to EF–X (4–9) P(2) band system (reported in Dabrowski & Herzberg (1976) at 1333.08485). The term values of the upper levels involved, B(11, 1) and EF(4, 1), are reported in Table 4 and separated by 8.76 reciprocal centimeters as already emphasised in Sect. 4.1.2. This suggests that some coupling between B and EF can take place and induce intensity anomalies. We then use a 2-state approximation and derive the coupling from the difference between the level energies. We may then evaluate the electronic weight factors corresponding to each state and derive the intensity of the two transitions: 60% of the total intensities are attributed to the B–X (11–9) P(2) and 40% to EF–X (4–9) P(2). This simple treatment allows the experimental fluorescence spectrum around 1333 Å to be explained. Other anomalies implying these same upper levels are expected in the whole spectrum.

5. Conclusion and summary

We give below a detailed description of the tables whose numerical data may be obtained in electronic form. The transition wavenumbers are accurate within a few wavenumbers,

Table 9. Properties of $C^{-1}\Pi_u$ rovibrational states: electronic weight factors, term value, total spontaneous emission probability (s^{-1}) and total dissociation probability (s^{-1}). Full table available in electronic form at the CDS.

v	ν	J	$\rho(C)$	$\rho(D)$	E cm^{-1}	A_t s^{-1}	A_c s^{-1}
0	1	1	1.00E+00	1.23E-06	99 275.91	1.18E+09	7.61E-04
1	2	1	1.00E+00	3.97E-06	101 289.54	1.16E+09	4.57E-04
2	3	1	1.00E+00	6.19E-06	103 202.15	1.15E+09	1.84E-02

Table 10. Properties of $D^{-1}\Pi_u$ rovibrational states: electronic weight factors, term value, total spontaneous emission probability (s^{-1}) and total dissociation probability (s^{-1}). Full table available in electronic form at the CDS.

v	ν	J	$\rho(C)$	$\rho(D)$	E cm^{-1}	A_t s^{-1}	A_c s^{-1}
0	10	1	2.06E-06	1.00E+00	113 064.46	3.56E+08	3.25E-03
1	13	1	4.85E-06	1.00E+00	115 006.08	3.51E+08	5.65E+00
2	16	1	2.78E-04	1.00E+00	116 850.05	3.46E+08	1.95E+05

Table 11. Spontaneous emission probabilities and transition wavenumbers of B–X (Lyman) band transitions of HD. Full table available in electronic form at the CDS.

v'	J'	v''	J''	A s^{-1}	σ cm^{-1}	o–c cm^{-1}	mn
0	0	0	1	4.177E+06	90 310.94	–	10
0	0	1	1	3.316E+07	86 682.63	–	10
0	0	2	1	1.204E+08	83 231.90	–0.60	11
0	0	3	1	2.664E+08	79 954.74	–0.52	11

Table 12. Spontaneous emission probabilities and transition wavenumbers of C^{+} –X (Werner) band transitions (P and R branches) of HD. Full table available in electronic form at the CDS.

v'	J'	v''	J''	A s^{-1}	σ cm^{-1}	o–c cm^{-1}	mn
0	1	0	0	7.130E+07	99 276.56	0.40	11
0	1	0	2	4.215E+07	99 009.44	–0.03	11
0	1	1	0	2.126E+08	95 644.40	–	10
0	1	1	2	1.200E+08	95 388.86	–	10

Table 13. Spontaneous emission probabilities and transition wavenumbers of B'–X band transitions of HD. Full table available in electronic form at the CDS.

v'	J'	v''	J''	A s^{-1}	σ cm^{-1}	o–c cm^{-1}	mn
0	0	0	1	1.480E+07	110 544.25	–1.29	11
0	0	1	1	6.204E+07	106 915.94	–	10
0	0	2	1	1.090E+08	103 465.21	–	10
0	0	3	1	1.047E+08	100 188.05	–	10

Table 14. Spontaneous emission probabilities and transition wavenumbers of D^{+} –X bands of HD. Full table available in electronic form at the CDS.

v'	J'	v''	J''	A s^{-1}	σ cm^{-1}	o–c cm^{-1}	mn
0	1	0	0	1.720E+07	113 066.22	0.54	14
0	1	0	2	1.025E+07	112 799.10	0.58	14
0	1	1	0	5.518E+07	109 434.06	–	10
0	1	1	2	3.330E+07	109 178.52	–	10

Table 15. Spontaneous emission probabilities and transition wavenumbers of C⁻-X (Werner) band transitions (Q branches) of HD. Full table available in electronic form at the CDS.

v'	J'	v''	J''	A s ⁻¹	σ cm ⁻¹	o-c cm ⁻¹	mn
0	1	0	1	1.134E+08	99 186.68	-0.04	11
0	1	1	1	3.326E+08	95 558.37	-	10
0	1	2	1	3.928E+08	92 107.64	-	10
0	1	3	1	2.418E+08	88 830.48	-0.38	11

Table 16. Spontaneous emission probabilities and transition wavenumbers of D⁻-X bands of HD. Full table available in electronic form at the CDS.

v'	J'	v''	J''	A s ⁻¹	σ cm ⁻¹	o-c cm ⁻¹	mn
0	1	0	1	2.745E+07	112 975.22	-	10
0	1	1	1	8.850E+07	109 346.91	-	10
0	1	2	1	1.168E+08	105 896.18	-	10
0	1	3	1	8.189E+07	102 619.02	-	10

and experimental values should be used when available. The transition probabilities are probably accurate within a few percent, and they update the previous calculations of Allison & Dalgarno (1969).

5.1. Tables 5–10

Tables 5–8 display the properties of the excited rovibronic levels of e -parity states linked by rotational and radial coupling, i.e. B ¹ Σ_u^+ , C ¹ Π_u^+ , B' ¹ Σ_u^+ and D ¹ Π_u^+ . As these states are coupled, we have labelled them according to the B.O. state of greatest electronic weight factor. Note that there is no coupling with C⁺ and D⁺ when $J = 0$, as the corresponding levels do not occur in Π electronic symmetry.

Column 1 gives the vibrational number.

Column 2 gives the energy order of the e -parity levels of the same J value irrespective of the label B, C, B', or D.

Column 3 gives the rotational quantum number.

Columns 4–8 give the fractions of B.O. state as defined in Sect. 2, Eq. (1).

Column 8 gives the term value.

Column 9 gives the total emission probability towards X ground electronic state in s⁻¹.

Column 10 gives the total dissociation probability towards X continuum in s⁻¹.

Tables 9–10 display the properties of the excited rovibronic levels of f -parity states that are coupled via radial coupling only between C ¹ Π_u^- and D ¹ Π_u^- . As for e levels, we have labelled them according to the B.O. state of greatest electronic weight factor.

Column 1 gives the vibrational number.

Column 2 gives the energy order of the f -parity levels of the same J value irrespective of the label C or D.

Column 3 gives the rotational quantum number.

Columns 4–5 give the fractions of B.O. state as defined in Sect. 2, Eq. (1).

Column 6 gives the term value.

Column 7 gives the total emission probability towards X ground electronic state in s⁻¹.

Column 8 gives the total dissociation probability towards X continuum in s⁻¹.

5.2. Tables 11 to 16

Tables 11 to 16 display the transition emission probabilities and transition wavenumbers towards X states for upper rotational quantum numbers less than 11. Comparison with experimental wavenumbers are given when available. The conventions to experimental references have been defined in Sect. 3.2.

The 14414 R and P transitions of the Lyman system (B–X) are displayed in Table 11, the 4778 R and P transitions of the Werner system (C–X) in Table 12, the 3213 R and P transitions of the B'–X system in Table 13, the 933 R and P transitions of the D–X system in Table 14, the 2482 Q transitions of the Werner system (C–X) in Table 15 and the 3257 Q transitions of the D–X system in Table 16.

Column 1 gives the upper vibrational quantum number v' .

Column 2 gives the upper rotational quantum number J' .

Column 3 gives the lower vibrational quantum number v'' .

Column 4 gives the lower rotational quantum number J'' .

Column 5 gives the presently calculated emission probabilities in s⁻¹.

Column 6 gives our obtained transition energies in cm⁻¹.

Column 7 gives o-c in cm⁻¹ when available.

Column 8 is a code mn, defined in Sect. 3.2, specifying which experimental reference has been used.

References

- Abgrall, H., Roueff, E., Launay, F., Roncin, J. Y., & Subtil, J. L. 1993, J. Molec. Spectrosc., 157, 512
- Abgrall, H., Roueff, E., Launay, F., & Roncin, J. 1994, Canadian J. Phys., 72, 856
- Abgrall, H., Roueff, E., Liu, X., Shemansky, D. E., & James, G. K. 1999, J. Phys. B Atom. Molec. Phys., 32, 3813

- Abgrall, H., Roueff, E., & Drira, I. 2000, *A&AS*, 141, 297
- Ajello, J., Vatti Palle, P., Abgrall, H., Roueff, E., Bhardwaj, A., & Gustin, J. 2005, *ApJS*, 159, 314
- Allison, A. C., & Dalgarno, A. 1969, *Atomic Data*, 1, 289
- André, M. K., Le Petit, F., Sonnentrucker, P., et al. 2004, *A&A*, 422, 483
- Dabrowski, I., & Herzberg, G. 1976, *Canadian J. Phys.*, 54, 525
- de Lange, A., Reinhold, E., Hogervorst, W., & Ubachs, W. 2000, *Canadian Journal of Physics*, 78, 567
- Dehmer, P. M., & Chupka, W. A. 1983, *J. Chem. Phys.*, 79, 1569
- Dressler, K., & Wolniewicz, L. 1986, *J. Chem. Phys.*, 85, 2821
- Hinnen, P. C., Werners, S. E., Stolte, S., Hogervorst, W., & Ubachs, W. 1995, *Phys. Rev. A*, 52, 4425
- Johnson, B. R. 1978, *J. Chem. Phys.*, 69, 4678
- Lacour, S., André, M. K., Sonnentrucker, P., et al. 2005, *A&A*, 430, 967
- Liu, X., Shemansky, D. E., Abgrall, H., et al. 2002, *ApJS*, 138, 229
- Liu, X., Shemansky, D. E., Abgrall, H., et al. 2003, *J. Phys. B Atom. Molec. Phys.*, 36, 173
- Monfils, A. 1965, *J. Molecular Spectroscopy*, 15, 265
- Reinhold, E., Hogervorst, W., Ubachs, W., & Wolniewicz, L. 1999, *Phys. Rev. A*, 60, 1258
- Senn, P., Quadrelli, P., & Dressler, K. 1988, *J. Chem. Phys.*, 89, 7401
- Staszewska, G., & Wolniewicz, L. 2002, *J. Molec. Spectrosc.*, 212, 208
- Takezawa, S., & Yanaka, Y. 1972, *J. Chem. Phys.*, 56, 6125
- Wolniewicz, L. 1993, *J. Chem. Phys.*, 99, 1851
- Wolniewicz, L. 1995, *J. Chem. Phys.*, 103, 1792
- Wolniewicz, L., & Dressler, K. 1988, *J. Chem. Phys.*, 88, 3861
- Wolniewicz, L., & Staszewska, G. 2003a, *J. Molec. Spectrosc.*, 217, 181
- Wolniewicz, L., & Staszewska, G. 2003b, *J. Molec. Spectrosc.*, 220, 45
- Wright, E. L., & Morton, D. C. 1979, *ApJ*, 227, 483